PAPER

Single ion solid-state composite electrolytes with high electrochemical stability based on a poly(perfluoroalkylsulfonyl)–imide ionene polymer†

Qianru Shi,[a] Lixin Xue,*[a] Dejun Qin,[a] Bing Du,[a] Jian Wang[a] and Liquan Chen[b]

Composite single ion solid-state polymer electrolytes were prepared by blending lithiated poly(perfluoroalkylsulfonyl)imide (PFSILi) ionene with poly(ethylene oxide) (PEO) at various PFSILi contents. Their electrochemical performance was characterized by ionic conductivity, lithium ion transport number, cyclic voltammetry and galvanostatic cycling in batteries. The composite PEO–PFSI-25, containing 24.5% of PFSI, was found to have a maximum ionic conductivity of 1.76×10^{-4} S cm^{-1} at 80 °C. Because of the immobilization of the anionic perfluorosulfonimide groups on the backbone of the ionene polymer with flexible and stable perfluoroether connectors, the composite had unusually high electrochemical stability (up to 5.5 V vs. Li$^+$/Li) and a low anion transference number. The PFSILi unit interacts strongly with the PEO segments, resulting in the depression of PEO crystallization and the formation of multi-dimensional ionic crosslinks within the composite to impart dimensional and cycling stability to the electrolyte system. LiFePO$_4$/Li battery prototypes using PEO–PFSILi polymer electrolytes, with reversible capacity of 140 mA h g^{-1} at 80 °C and 0.2 °C, were able to maintain 50 stable cycles for 1000 h at 70 °C and 0.1 °C.

1. Introduction

Lithium (Li) metal is an attractive contender for use as the anode in high energy and high capacity power sources, including Li–sulfur[1] and Li–air batteries,[2,3] because of its high theoretical specific capacity (3860 mA h g^{-1}), low electrochemical potential (−3.04 V vs. a standard hydrogen electrode) and low density (0.59 g cm^{-3}).[4] Rechargeable lithium batteries have been considered as the next generation power sources for electric vehicles or hybrid electric vehicles because of their high energy and power capability.[5,6] However, even state-of-the-art lithium batteries barely satisfy the energy or capacity requirements to allow vehicles to travel as far as 350 km.[7] Current lithium batteries usually suffer from poor cycling performance, and there are safety issues related to the formation of dendrite metal during the cycles and the leaking of liquid electrolytes.[8–10] Solid-state polymer electrolytes (SPEs), comprising a polar polymer matrix and lithium salts,[11,12] have been proposed for replacing liquid electrolytes and to lessen the dendrite growth forming mechanical barriers.[13–15] It is believed that the use of SPEs could resolve the safety and long-term stability issues currently associated with lithium-based batteries.[16]

In a typical SPE system containing poly(ethylene oxide) (PEO) and the lithium salt of bis(trifluoromethanesulfonyl)imide (LiTFSI),[17] lithium ions are complexed with the oxygen atoms in the PEO chains. Ionic conduction is assisted by the segmental motion of the flexible PEO chains in the amorphous regions, but the crystallization of PEO chains may hamper the segmental motion and lead to low ionic conductivity.[18,19] Attempts have therefore been made, including crosslinking, or the addition of plasticizers or nano-size ceramic fillers, to suppress the crystallization of PEO chains in PEO–lithium salt electrolyte systems.[20]

The lithium ion transference numbers (t^+) for the polymer–lithium salt systems are generally below 0.5, because of the movable small anions that are present. High anionic motion in lithium batteries may cause high polarization, limited power delivery and premature cell failure.[21] Ionic conductors with a poly-anionic structure and based on comb-like polymers, network polymers and composites have been reported to have high lithium ion transference numbers.[22,23] In these polymers, high cationic conductivity can be achieved by incorporating super-acidic functional groups, such as the perfluoroalkylsulfonimide group.

Polymers containing perfluoroalkylsulfonimide (PFSI) groups have been systematically studied by DesMarteau[24–26] and

*a*Ningbo Institute of Materials Technology & Engineering, Chinese Academy of Sciences, Ningbo, 315201, China. E-mail: xuelx@nimte.ac.cn; Tel: +86-0574-86688271

*b*Institute of Physics, Chinese Academy of Sciences, Beijing, 100190, China

Watanabe,[27,28] and Meziane et al. recently introduced a composite SPE based on poly[(4-styrenesulfonyl)(trifluoromethanesulfonyl)imide] anions (P(STFSILi)) and PEO.[29] Single lithium-ion conducting polymer electrolytes based on a P(STFSILi) and methoxy-polyethylene glycol acrylate blend have also been reported.[30] However, the rigid unsaturated C=C bonds in the polymer structure may limit their long-term cycling performance because of their poor compatibility and stability in the PEO matrix.[31] A series of lithium polyanionic salts based on LiTFSI units, connected by perfluoroalkane linkers and using PEO as the polymer host, have been studied as SPEs, and the properties of polyanionic chains of variable length have been carefully investigated, including ionic conductivity, cationic transference number, and salt diffusion coefficients.[32,33]

Recently, our own group has been working on the synthesis and applications of lithium poly(perfluoroalkylsulfonyl)imide (PFSILi) ionene polymers. These non-aromatic lithiated ionene polymers have a backbone of perfluoroalkylsulfonimide groups, providing a low lithium dissociation energy and a high cationic exchange capacity of about 2.9 meq. g^{-1}. In a previous study, PFSILi blends with polyvinylidene fluoride (PVDF) were effective as electrode binders in reducing the polarization of lithium batteries at higher cycling rates,[34] the idea being to develop novel ionene-based polymer electrolytes containing the flexible stable perfluoroether connector, $-CF_2CF_2OCF_2CF_2-$, which can maintain high lithium ion transport number and ionic conductivity. Without an unsaturated rigid aromatic structure, this may give high electrochemical stability and better compatibility with PEO. In the present study the performance of PEO–PFSILi composite polymer electrolytes at various compositions has been evaluated by studying their ionic conductivity, lithium ion transport number, electrochemical stability and galvanostatic cycling in batteries.

2. Materials and methods

2.1 Preparation of solid polymer electrolytes

Solid electrolyte membranes were produced by casting. PFSILi was produced and characterized by a method previously published. After drying under vacuum for 24 h, PFSILi and PEO (Aldrich) were dissolved in dry acetonitrile (HLPC grade, Aladdin, China) for 24 h in proportions ranging from 21 to 50 wt% PFSILi (Table 1). The mixture was cast on a Teflon plate inside a dry box and left to stand at room temperature for 24 h to allow the acetonitrile to evaporate. The membrane was

further dried under vacuum for 25 h at 40 °C and then stored in an argon-filled glove box.

2.2 Characterization

A symmetrical stainless steel/PEO–PFSILi/stainless steel cell was assembled to determine the ionic conductivity by using a two electrode AC impedance method. The measurements were conducted on a Zahner Zennium EL101 electrochemical station over a frequency range from 100 mHz to 100 MHz with a disturbing voltage of 10 mV within the temperature range 20 to 80 °C. At each temperature the cell was stabilized for 1 h before testing.

Cyclic voltammetry (CV) measurements were carried out to determine the electrochemical stability window in the lithium/PEO–PFSILi/stainless-steel cells between −1 and 6 V at a rate of 1 mV s^{-1}. The cells were heated at 70 °C for 2 h to reach equilibrium.

For battery testing, LiFePO$_4$/PEO–PFSILi/lithium batteries were assembled using a lamination process in 2032 coin-type cells. The cathode comprised 80 wt% LiFePO$_4$ (Advanced Lithium Ion Battery Engineering Laboratory, at the Ningbo Institute of Materials Technology and Engineering), 10 wt% Super P (Timcal, Switzerland) and 10 wt% PVDF binder (HSV 900, Arkema Co. Ltd, France). Battery cycling experiments were performed on a Landt CT2001A battery tester between 2.7 and 4.2 V (1 C is 0.665 mA cm^{-2}, corresponding to the theoretical capacity of the LiFePO$_4$ cathode, 170 mA h g^{-1}).

The calorimetric measurements were performed on a differential scanning calorimeter (DSC, Mettler Toledo Star System) using a heat–cool–heat cycle from −30 to 100 °C under a nitrogen flow. The heating rate was 10 °C min^{-1} and the cooling rate 5 °C min^{-1}.

Atomic force microscopy (AFM) phase images of PEO–PFSILi were obtained on a BenYuan CSPM5500 microscope in tapping mode using the standard etched silicon probe tip. All the images were scanned at a frequency of 1.5 Hz. Each scan line contained 512 pixels, and the complete image was composed of 512 scan lines.

3. Results and discussion

3.1 Ionic conductivity

The ionic conductivities of the polymer–electrolyte composites: PEO–PFSILi-30, -25, -20, -16 and -8 with various PFSILi contents (21, 24.5, 29, 33 and 50 wt%, respectively) are illustrated in Fig. 1. In the temperature region above the melting point of PEO, PEO–PFSILi-25 showed a maximum ionic conductivity of 1.76×10^{-4} S cm^{-1} at 80 °C. The phenomenon of maximum conductivity occurring at a medium salt concentration is consistent with previous studies,[35] and has been ascribed to the synergistic effect between the ionic dissociation and hopping between the PFSILi chains and PEO chain segments.[36,37] At low PFSILi content the ionic conductivity may be limited by the low concentration of lithium ions, and at high PFSILi content by the lack of amorphous PEO chains to facilitate cationic motion.[38] The high lithium ion transport number of 0.90, calculated by
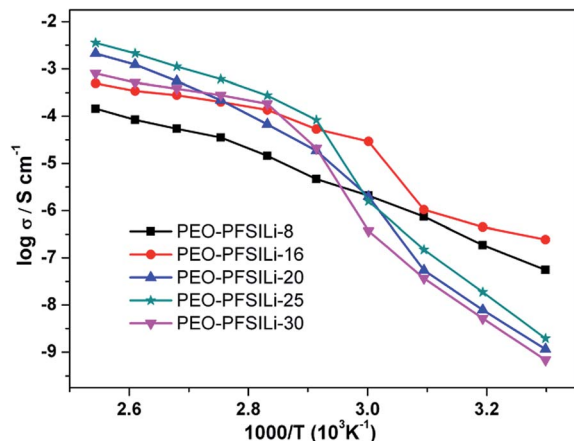
Table 1 Composition of PEO–PFSILi blends

Sample	M_n (PEO) g mol^{-1}	M_n (PFSILi) g mol^{-1}	Wt% of PFSILi	[EO] : [Li$^+$]
PEO–PFSI-8	60 000	21 000	50%	8 : 1
PEO–PFSI-16			33.3%	16 : 1
PEO–PFSI-20			28.9%	20 : 1
PEO–PFSI-25			24.5%	25 : 1
PEO–PFSI-30			21%	30 : 1

Fig. 1 Arrhenius plots of conductivity as a function of temperature for PEO–PFSILi solid electrolyte composites.

Fig. 2 DSC of PEO–PFSILi solid electrolytes at a temperature ramp rate of 5 °C min⁻¹.

the Bruce–Evans–Vincent method (ESI Table S1†), characterizes the single-ion conduction behavior of the solid-state electrolyte.

Regarding the crystallization of PEO polymeric chains at around 60 °C, a clear turning point in the temperature region 50–70 °C was observed in the Arrhenius plots of ionic conductivity for compositions PEO–PFSILi-30, -25 and -20, representing a structural change in the ionic conducting channels. When the membranes were cooled down at high PEO content an excess of PEO chains crystallized, resulting in an increase in the ionic transfer activation energy and a decrease in ionic conductivity, as summarized in Table 2. For composition PEO–PFSILi-16, with a lower PEO and a higher PSFILi content of 33 wt%, there was no obvious increase in activation energy during the cooling process, although there was a dramatic drop in ionic conductivity between 60 and 50 °C. For composition PEO–PFSILi-8, with an even higher PFSILi content of 50 wt%, the turning point or drop in conductivity disappeared, indicating a complete halt to the crystallization of PEO chains because of a strong intermolecular interaction between the PFSILi and PEO molecules. This interaction was further confirmed by the disappearance of a crystalline peak in the DSC graph of PEO–PFSILi-8, shown in Fig. 2 and discussed below.

3.2 Thermal behaviour

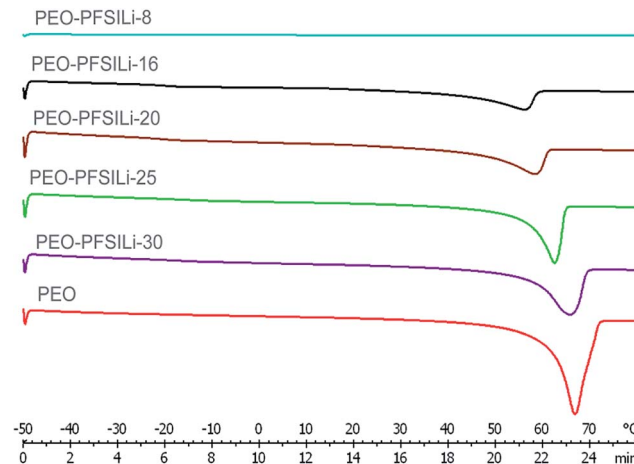The DSC was employed to characterize the thermal behavior of the composite electrolytes and study the effect of segment mobility on conductivity, as shown in Fig. 2 and Table 2. As discussed earlier, the addition of PFSILi could disrupt the order of the PEO segments, resulting in a lower degree of crystallization and decreased crystallization temperature, T_c. In the case of PEO–PFSILi-8, with a high PFSILi content of 50 wt%, the crystallinity peak disappeared, indicating a low degree of PEO crystallization at room temperature. The ionic conduction barriers formed by the crystallized PEO segments were thus totally eliminated, leading to relatively high ionic conductivity at a lower temperature, which is consistent with the ionic conductivity data listed in Fig. 1.

3.3 Electrochemical stability

The CV curve of PEO–PFSILi-25 presented in Fig. 3 may be used to characterize the electrochemical stability of the compositions. It is surprising to see that PEO–PFSILi-25 was stable up to 5.5 V, unlike Li⁺/Li, which is much more stable than traditional small salt-laden PEO composites, e.g., PEO–LiTFSI, shown for comparison in Fig. 4. This result agrees with the fact that the reduction in small mobile anions accumulating at the anodes could lead to the electrochemical instability of the system. As PFSILi has a poly-anionic structure, the anions are anchored and can avoid migration. Thus, only anions at the interface with

Table 2 Property data for PEO–PFSILi composites

Sample	PFSILi wt%	Ea1 kJ mol⁻¹	Ea2 kJ mol⁻¹	σ turning °C	T_c °C	Hf (PEO) J g⁻¹	Crystallinality[a] %
PEO–PFSI-8	50.0%	38.2	—	—	—	—	0.0%
PEO–PFSI-16	33.3%	17.5	19.5	50–60	56.1	72.0	33.6%
PEO–PFSI-20	28.9%	68.2	53.6	50–60	58.3	79.8	37.2%
PEO–PFSI-25	24.5%	80.6	35.8	60–70	62.4	95.3	44.4%
PEO–PFSI-30	21.0%	76.1	30.6	60–80	65.5	96.0	44.7%
PEO	—	—	—	—	66.5	144.6	67.4%

[a] Calculated from the reference melting enthalpy of 214.6 J g⁻¹ for PEO with 100% crystallinity.

15954 | J. Mater. Chem. A, 2014, 2, 15952–15957

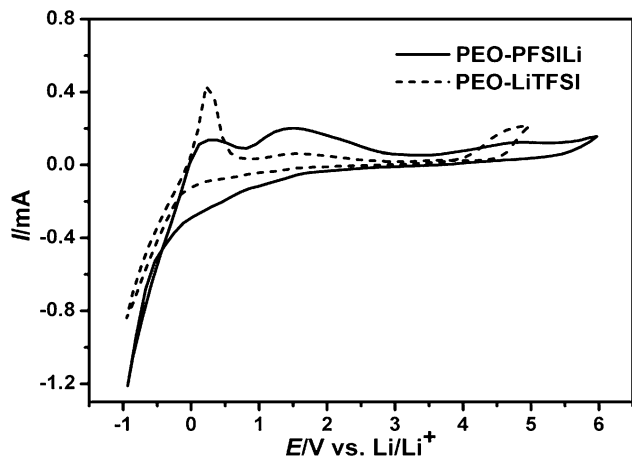This journal is © The Royal Society of Chemistry 2014

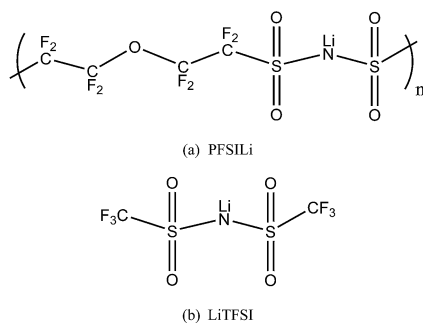Fig. 3 Cyclic voltammograms of PEO–PFSILi-25 vs. PEO–LiTFSI. Scanning rate: 10 mV s^{-1}.

Fig. 4 Structures of (a) PFSILi and (b) LiTFSI.

the electrodes may lose negative charge, leading to enhanced electrochemical stability.[11,39]

In this case, the absence of non-saturated bonds in the poly-anionic structure of PFSILi also adds to its electrochemical stability. The performance of previously reported composite single lithium ion-conducting polymer electrolytes based on P(STFSILi)[17,18] might have been limited by the presence of rigid unsaturated benzene rings in their structures and the ineffective mixing of the rigid structure with soft PEO. Current PFSILi ionenes exhibit a high degree of Li cation dissociation, as well as flexible and stable perfluoroether connectors ($-CF_2CF_2OCF_2CF_2-$), and have compatibility and stability in a PEO matrix, leading to less boundary polarization and higher long-term electrochemical stability. Furthermore, in comparison to the lithium salt, LiTFSI, PFSILi is a type of single lithium-ion conducting polymer with perfluoroether connectors, and this structure is less mobile, because of the interaction between or within the polymer chains as well as interaction with the PEO chains. During the charging and discharging process, it is only the Li cation that moves to the electrode and engages in the oxide-reduction reaction. For LiTFSI, both the Li cation and TFSI anion move to the electrodes, and a number of side reactions may take place there. Therefore, the polymer structure PFSILi exhibits better electrochemical stability.

3.4 Battery test

To test the feasibility of using the novel single ion composite PEO–PFSILi-25 as a solid-state electrolyte for rechargeable lithium batteries, we assembled and tested the button battery prototypes using typical LiFePO$_4$ cathodes and lithium metal anodes. The cycling test on the LiFePO$_4$/PEO–PFSILi/Li battery was performed in the voltage range between 2.7 and 4.2 V at temperatures of 70 °C and 80 °C, at rates of 0.1 and 0.2 °C.

According to the results summarized in Fig. 5, at a charge and discharge rate of 0.1 °C the performance of solid-state PEO–PFSILi-25 electrolyte at 70 °C could approach that of common liquid electrolytes running in cells at room temperature. At the 0.1 °C rate and 70 °C, the discharge capacity of the cell was stable at around 150 mA h g^{-1}, with a discharge plateau potential around 3.4 V. Fig. 6 illustrates the long-term stability of the LiFePO$_4$/Li polymer cell using PEO–PFSILi-25 as electrolyte. The cell was successfully cycled at 70 °C and 0.1 °C for more than 50 cycles over a period of 50 days. It is interesting to see that for the first 30 cycles, the discharge capacity was maintained above 140 mA h g^{-1}, 82% of the theoretical specific capacity. Even at the end of the 50th cycle, the capacity was still above 120 mA h g^{-1}. Bearing in mind that the present button cell can operate even after accelerated ageing at high temperature for over 1000 h, it may be considered to offer excellent long-term stability.

To cycle lithium batteries based on composite, solid-state polymer electrolytes at rates above 0.2 °C was quite a challenge. As shown in Fig. 5, when the rate was increased to 0.2 °C at 70 °C the capacity of the cell dropped to 110 mA h g^{-1} and the discharge plateau to below 3.3 V. Although the capacity of the cell at a rate of 0.2 °C could be improved to above 135 mA h g^{-1} by increasing the operating temperature to 80 °C, the discharge plateau fell further to below 3.2 V. This may be attributed to slower Li cation migration kinetics at the inter-phase boundaries under higher charge and discharge rates in the dry heterogeneous system. The situation may be clarified in future studies by preparing a multi-blocked homogenous co-polymeric electrolyte system.[38]

Briefly, the composite, solid-state electrolyte PEO–PFSILi could be used as an effective single-ion conductor for lithium batteries with reasonably good performance at rates of 0.1 and 0.2 °C. As shown in Table 3, the LiFePO$_4$/Li battery tested with PEO–PFSILi outperformed the reported heterogeneous composite electrolytes, including PEO–LiCF$_3$SO$_3$,[41] PEO$_{20}$-LiCF$_3$SO$_3$-Al$_2$O$_3$-ST[41] or PSF–PEO-LiTFSI-succinonitrile[42] electrolytes. It is likely in future studies that the performance of the reported homogenous tri-block electrolyte copolymer will be investigated,[38] if the boundary polarization in the electrodes or between phases can be reduced.

3.5 Phase image

The stable cycling indicated that the PEO–PFSILi electrolyte had a sufficiently stable structure to sustain the repeat volume variations in active materials during the charge–discharge process over a long period. To verify this, AFM was used to study the phase image between the PEO–PFSILi and PEO–LiTFSI
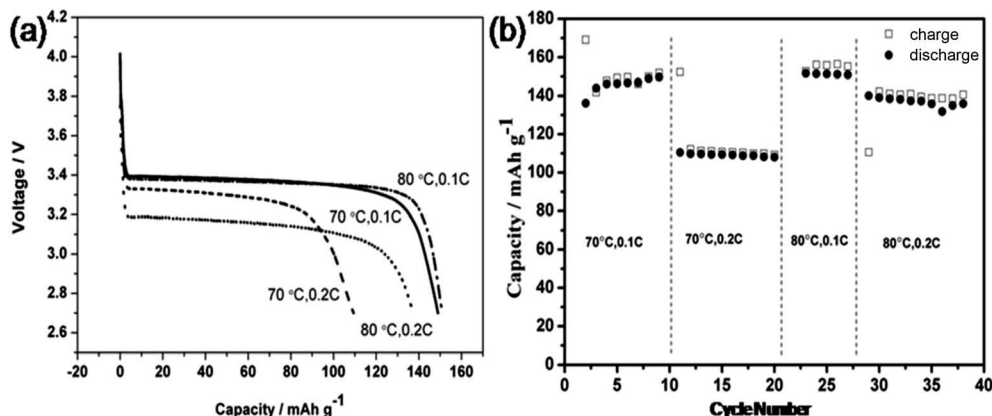
Fig. 5 (a) Discharge voltage profile, and (b) cycling performance of the LiFePO$_4$/Li cell with a solid polymer electrolyte at 70 and 80 °C at a rate of 0.1 and 0.2 °C.
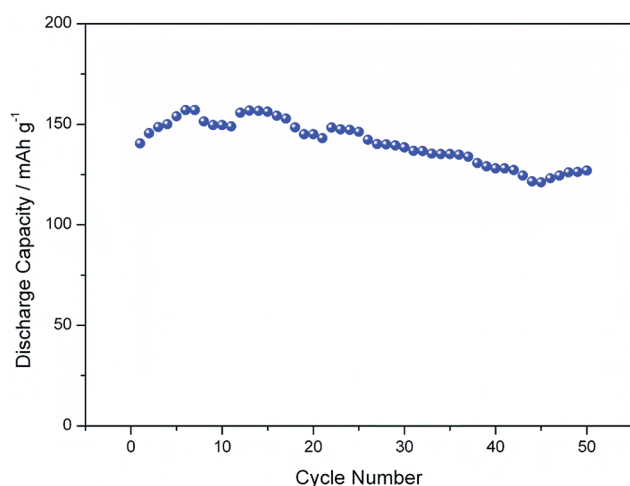

Fig. 6 Long-term cycling stability of a LiFePO$_4$/Li cell with PEO–PFSILi-25 solid polymer electrolyte at a temperature of 70 °C and a rate of 0.1 °C.
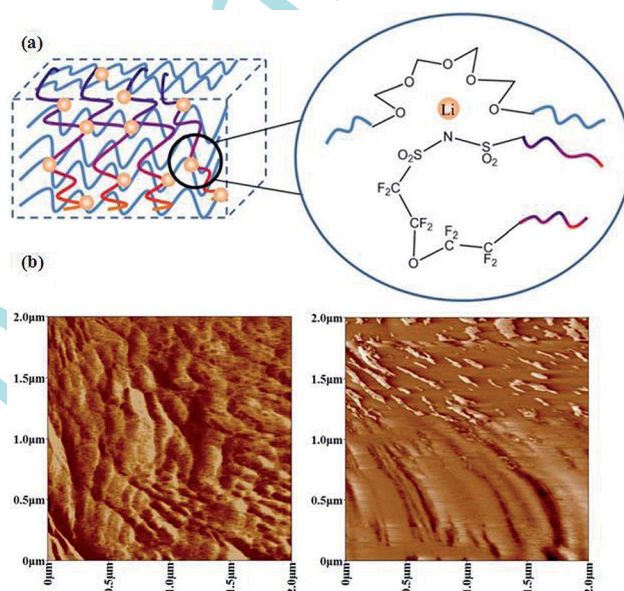

Fig. 7 (a) Illustration of the PEO–PFSILi solid electrolyte configuration; (b) AFM phase images of PEO–PFSILi (left) and PEO–LiTFSI (right).

electrolytes. As shown in Fig. 7(b), unlike the sharp phase separation observed in PEO–LiTFSI, the PEO–PFSILi composite showed well-merged knitted inter-phase networks. This was because of the presence of the ethylene oxide (EO) units in the PEO chain, which were favorably coordinated with the lithium ions by the electron donor oxygen atom, the lithium ions becoming ionic crosslinkage sites between the PEO chain and the PFSILi chain. The flexible structure of PEO and PFSILi are easily interpenetrated and the ionic crosslinkage fixes the network structure further. This type of crosslinkage is constructed by ionic crosslinkage instead of by covalent bonding, and the degree of ionic crosslinking is dynamic and varies during the ion transfer process. It seems that the ionene

polymer chains, with polyanions connected by flexible perfluoroether connectors, $-CF_2CF_2OCF_2CF_2-$, could become fully entangled with the PEO chains by ionic bridging, forming multi-dimensional ionic crosslinkages, as illustrated in Fig. 7(a). This multi-dimensional crosslinked structure enhances the dimensional stability of the SPE at high temperatures over the longer term. This improved dimensional stability not only sustains the volume change caused by the electrode materials, but also prevents the growth of lithium metal dendrites during cycling.

Table 3 Comparison of cell performance of LiFePO$_4$/Li cells with PEO–PFSILi and other reported solid electrolytes, in ref. 38–40

Sample	PEO–PFSILi	PEO–LiCF$_3$SO$_3$ (ref. 39)	PEO–LiCF$_3$SO$_3$–ceramic[39]	PSF–PEO–LiTFSI[40]	Copolymer[38]
Environment	80 °C, 0.2 °C	90 °C, 0.2 °C	90 °C, 0.2 °C	80 °C, 0.2 °C	80 °C, 0.25 °C
Capacity (mA h g^{-1})	140	100	130	120	150

15956 | J. Mater. Chem. A, 2014, 2, 15952–15957

This journal is © The Royal Society of Chemistry 2014

4. Conclusions

A novel type of single ion solid polymer electrolyte was developed by blending lithiated poly(perfluoroalkylsulfonyl)imide ionene with polyethylene oxide to give excellent electrochemical properties in terms of ionic conductivity (1.76×10^{-4} S cm^{-1} at 80 °C), lithium ion transport number (0.908) and electrochemical stability (up to 5.5 V vs. Li$^+$/Li). Because of interaction between the flexible ionene polymer and the PEO segments, multi-dimensional ionic crosslinkages were formed inside the electrolyte structure, resulting in enhanced dimensional and long-term electrochemical stability. A LiFePO$_4$/Li cell with a PEO–PFSILi solid electrolyte showed high capacity and excellent long-term cycling stability: over 1000 h at 70 °C and 0.1 °C. The PEO–PFSILi composite solid-state single ion-conducting polymer electrolyte is attractive for its exceptionally high electrochemical stability, and has potential applications in rechargeable lithium batteries running at higher voltages.

References

1   J. Hassoun and B. Scrosati, *Angew. Chem., Int. Ed.*, 2010, **49**, 2371.

2   S. A. Freunberger, Y. Chen, N. E. Drewett, L. J. Hardwick, F. Barde and P. G. Bruce, *Angew. Chem., Int. Ed.*, 2011, **50**, 8609.

3   P. G. Bruce, S. A. Freunberger, L. J. Hardwick and J.-M. Tarascon, *Nat. Mater.*, 2012, **11**, 19.

4   M. M. Thackeray, C. Wolverton and E. D. Isaacs, *Energy Environ. Sci.*, 2012, **5**, 7854.

5   A. Yoshino, *Angew. Chem., Int. Ed.*, 2012, **51**, 5798.

6   M. Armand and J. M. Tarascon, *Nature*, 2008, **451**, 652.

7   J. M. Tarascon and M. Armand, *Nature*, 2001, **414**, 359.

8   F. Ding, W. Xu, G. L. Graff, J. Zhang, M. L. Sushko, X. Chen, Y. Shao, M. H. Engelhard, Z. Nie, J. Xiao, X. Liu, P. V. Sushko, J. Liu and J.-G. Zhang, *J. Am. Chem. Soc.*, 2013, **135**, 4450.

9   M. Dollé, L. Sannier, B. Beaudoin, M. Trentin and J.-M. Tarascon, *Electrochem. Solid-State Lett.*, 2002, **5**, A286.

10 J. Wen, Y. Yu and C. Chen, *Mater. Express*, 2012, **2**, 197.

11 M. Armand, *Solid State Ionics*, 1983, **9–10**, 745.

12 M. Armand, *Solid State Ionics*, 1994, **69**, 309.

13 C. Brissot, M. Rosso, J. N. Chazalviel, P. Baudry and S. Lascaud, *Electrochim. Acta*, 1998, **43**, 1569.

14 C. Brissot, M. Rosso, J. N. Chazalviel and S. Lascaud, *J. Power Sources*, 1999, **81**, 925.

15 T. Osaka and T. Momma, *J. Power Sources*, 2001, **97–98**, 765.

16 K. Murata, S. Izuchi and Y. Yoshihisa, *Electrochim. Acta*, 2000, **45**, 1501.

17 W. Gorecki, M. Jeannin, E. Belorizky, C. Roux and M. Armand, *J. Phys.: Condens. Matter*, 1995, **7**, 6823.

18 C. Do, P. Lunkenheimer, D. Diddens, M. Goetz, M. Weiss, A. Loidl, X.-G. Sun, J. Allgaier and M. Ohl, *Phys. Rev. Lett.*, 2013, **111**, 018301.

19 K. M. Abraham, Z. Jiang and B. Carroll, *Chem. Mater.*, 1997, **9**, 1978.

20 P. Jayathilaka, M. Dissanayake, I. Albinsson and B. E. Mellander, *Electrochim. Acta*, 2002, **47**, 3257.

21 M. Doyle, T. F. Fuller and J. Newman, *Electrochim. Acta*, 1994, **39**, 2073.

22 M. Kurian, M. E. Galvin, P. E. Trapa, D. R. Sadoway and A. M. Mayes, *Electrochim. Acta*, 2005, **50**, 2125.

23 D. Benrabah, S. Sylla, F. Alloin, J. Y. Sanchez and M. Armand, *Electrochim. Acta*, 1995, **40**, 2259.

24 D. D. Desmarteau, *J. Fluorine Chem.*, 1995, **72**, 203.

25 L. X. Xue, C. W. Padgett, D. D. DesMarteau and W. T. Pennington, *Solid State Sci.*, 2002, **4**, 1535.

26 L. X. Xue, D. D. DesMarteau and W. T. Pennington, *Angew. Chem., Int. Ed.*, 1997, **36**, 1331.

27 H. Tokuda, S. I. Tabata, M. Susan, K. Hayamizu and M. Watanabe, *J. Phys. Chem. B*, 2004, **108**, 11995.

28 A. Oishi, H. Matsuoka, T. Yasuda and M. Watanabe, *J. Mater. Chem.*, 2009, **19**, 514.

29 R. Meziane, J.-P. Bonnet, M. Courty, K. Djellab and M. Armand, *Electrochim. Acta*, 2011, **57**, 14.

30 S. Feng, D. Shi, F. Liu, L. Zheng, J. Nie, W. Feng, X. Huang, M. Armand and Z. Zhou, *Electrochim. Acta*, 2013, **93**, 254.

31 A. Kraytsberg and Y. Ein-Eli, *Adv. Energy Mater.*, 2012, **2**, 922.

32 O. Geiculescu, J. Yang, S. Zhou, G. Shafer, Y. Xie, J. Albright, S. Creager, W. Pennington and D. DesMarteau, *J. Electrochem. Soc.*, 2004, **151**, A1363–A1368.

33 O. E. Geiculescu, R. Rajagopal, S. E. Creager, D. D. DesMarteau, X. Zhang and P. Fedkiw, *J. Phys. Chem. B*, 2006, **110**, 23130–23135.

34 Q. Shi, L. Xue, Z. Wei, F. Liu, X. Du and D. D. DesMarteau, *J. Mater. Chem. A*, 2013, **1**, 15016.

35 S. Feng, D. Shi, F. Liu, L. Zheng, J. Nie, W. Feng, X. Huang, M. Armand and Z. Zhou, *Electrochim. Acta*, 2013, **93**, 254.

36 R. J. Klein, D. T. Welna, A. L. Weikel, H. R. Allcock and J. Runt, *Macromolecules*, 2007, **40**, 3990.

37 S. W. Ryu, P. E. Trapa, S. C. Olugebefola, J. A. Gonzalez-Leon, D. R. Sadoway and A. M. Mayes, *J. Electrochem. Soc.*, 2005, **152**, A158.

38 D. J. Bannister, G. R. Davies, I. M. Ward and J. E. McIntyre, *Polymer*, 1984, **25**, 1291.

39 M. Armand, *Adv. Mater.*, 1990, **2**, 278.

40 R. Bouchet, S. Maria, R. Meziane, A. Aboulaich, L. Lienafa, J. P. Bonnet, T. N. Phan, D. Bertin, D. Gigmes, D. Devaux, R. Denoyel and M. Armand, *Nat. Mater.*, 2013, **12**, 452.

41 B. W. Zewde, S. Admassie, J. Zimmermann, C. S. Isfort, B. Scrosati and J. Hassoun, *ChemSusChem*, 2013, **6**, 1400.

42 Q. Lu, J. Fang, J. Yang, G. Yan, S. Liu and J. Wang, *J. Membr. Sci.*, 2013, **425–426**, 105.

This journal is © The Royal Society of Chemistry 2014

J. Mater. Chem. A, 2014, **2**, 15952–15957 | **15957**